

## Studies of energy during strong and weak monsoon situations over India

S. N. PANDEY, J. CHATTOPADHYAY and U. S. SINGH

Dept. of Geophys., Banaras Hindu University, Varanasi

(Received 16 March 1988)

सार — पांच स्तरीय डायग्नोस्टिक मॉडल द्वारा विभिन्न दाबों पर भारत में प्रबल और दुर्बल मानसून स्थितियों के लिए ऊर्जा के आधारभूत रूपों, अर्थात्,  $A_Z$ ,  $A_E$ ,  $K_Z$  और  $K_E$  का परिकलन किया गया। उर्ध्वाधर एकीकृत दैनिक विभिन्नता के अनुसार मानसून की तीव्रता ऊर्जा के भंडार रूप की तीव्रता से संबंधित है।

ABSTRACT. The basic forms of energy, namely,  $A_Z$ ,  $A_E$ ,  $K_Z$  and  $K_E$  were computed for strong and weak monsoon situations over India at different pressures by a five-level diagnostic model. The vertically integrated daily variation suggests that the intensity of the monsoon is associated with the intensity of eddy form of energy.

### 1. Introduction

The strength of cyclones, anticyclones and other weather systems is measured by their kinetic energy. The weakening or strengthening of a system depends on whether it is losing or gaining kinetic energy. Consequently, the source or sink of energy becomes a matter of importance (Lorenz 1955). The potential and internal energy of the atmosphere under hydrostatic balance bears a constant ratio ( $R/c_p$ ), if we ignore the effect of ground terrain. Thus, the sum of the two is the total potential energy (TPE). Lorenz (1955) defined the available potential energy (APE) as the difference between TPE and the minimum TPE, which is obtained by adiabatic redistribution of mass. This can be further divided into two parts considering zonal motion and eddies. The former is the zonal available potential energy ( $A_Z$ ), while the eddy available potential energy ( $A_E$ ) refers to the latter. The total kinetic energy may be also resolved into zonal ( $K_Z$ ) and eddy kinetic energy ( $K_E$ ) respectively.

We will compute  $A_Z$ ,  $A_E$ ,  $K_Z$  and  $K_E$  over the Indian subcontinent for two different synoptic situations. They represent a strong monsoon situation (Case I), while the other represents a weak monsoon situation (Case II). Advection of energy has been also computed, and the results are discussed.

### 2. Method

2.1. For this purpose, we considered five input levels, namely, grid point geopotentials at 850, 700, 500, 300 and 200 mb over a limited area. Expressions for the

different variables are summarized in section 2.2. We also used the following expressions for the geostrophic wind and temperature fields :

$$p^a = RT \quad (1)$$

$$dp = -g\rho dz \quad (2)$$

$$T = (-g/R)(p\partial z/\partial p) \quad (3)$$

$$u_g = -(g/f)(\partial z/\partial y) \quad (4)$$

$$v_g = (g/f)(\partial z/\partial x) \quad (5)$$

A rectangular latitude/longitude grid with  $2.5^\circ$  resolution was selected. The area under computation extended from  $7.5^\circ$  N to  $30^\circ$  N and  $62.5^\circ$  E to  $97.5^\circ$  E. Along the zonal and meridional directions there were 15 and 10 grid points respectively. The data used for the computation at grid points were obtained from the operational objectively analysed geopotential heights of constant pressure surfaces by the India Meteorological Department using Cressman's technique at 850, 700, 500, 300 and 200 mb at 00 GMT each day. Shumans (1957) nine-point smoothing was used for filtering small scale fluctuations.

From these geopotentials over a three dimensional mesh, the first derivatives at the original input levels were obtained through a subroutine which utilized a cubic Spline interpolation scheme to derive the function and its derivatives at the original input level. The values of the function and its derivatives were linearly extrapolated at the lateral boundaries to find the temperature at each level by Eqn. (3). These temperatures are used to compute the stability factor,  $\gamma$ . The computed fields of  $T$  and  $\gamma$  were utilized to obtain the available potential energy (Sec. 2.2).

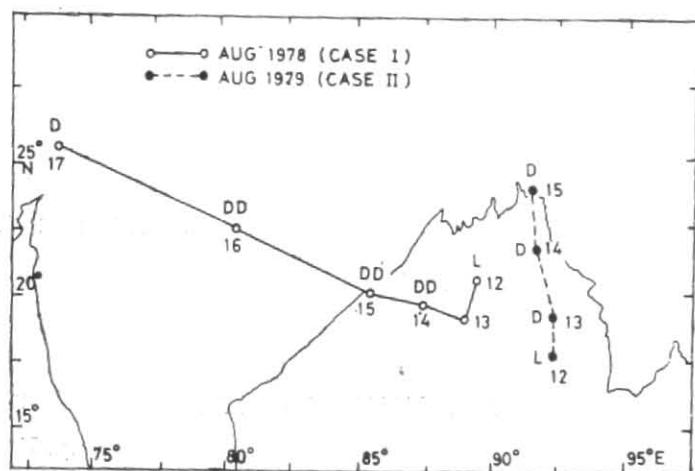


Fig. 1. Surface tracks of the depression for cases I and II

The wind components at each grid point were computed by Eqns. (4) and (5) using the geopotentials as input. Here the first derivatives were computed by a finite difference scheme. The computations were performed for the first derivatives up to one grid point interior to the outer boundaries over the area. At the boundaries the resulting values were linearly extrapolated. However, the first vertical derivatives, such as  $\partial T/\partial p$  at the lowest boundary, that is, 850 mb were calculated by extrapolation of the derivatives at 700 mb and 500 mb with weights of 1.5 and 0.5 respectively. A similar procedure was adopted to compute the first derivatives at the uppermost boundary, *i.e.*, 200 mb.

The tracks of the two depressions are shown in Fig. 1. From the figure we note that the centre of the 1978 depression passes along the Indo-Gangetic plain, which is the normal position of the monsoon trough. This northward movement of the depression along the monsoon trough made the monsoon active or vigorous throughout the period extending from 11 to 18 August 1978 over most parts of India. But, the 1979 depression track represents a northward shift of the monsoon trough towards the foothills of the Himalayas. This causes a weak monsoon situation over the subcontinent from 12 to 16 August 1979\*. These two situations were selected for the present study. The different energy terms for the complete life cycle of these two depressions were computed.

## 2.2. Basic equations

In line with Smagorinsky (1963) and Kida (1977), the following expressions were used for computation:

$$A_T = \int_M \frac{1}{2} \gamma (\overline{T''})^2 dM \quad (6)$$

$$A_Z = \int_M \frac{1}{2} \gamma (\overline{T''})^2 dM \quad (7)$$

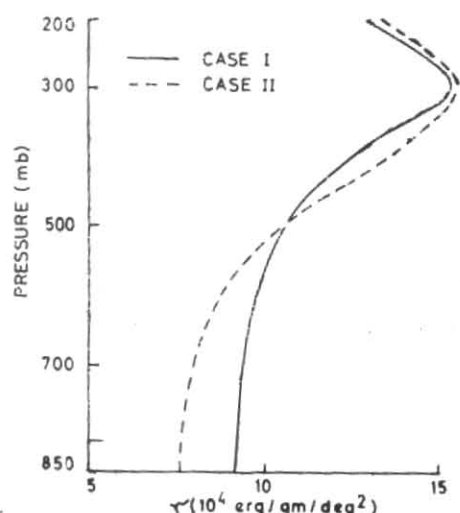


Fig. 2. Vertical variation of the stability factor for cases I and II

$$A_E = A_T - A_Z \quad (8)$$

$$\gamma = \frac{R}{p \left( \frac{\partial [T]}{\partial p} - \frac{R [T]}{c_p p} \right)} \quad (9)$$

$$K_T = \int_M \frac{1}{2} (u^2 + v^2) dM \quad (10)$$

$$K_Z = \int_M \frac{1}{2} (u^2 + v^2) dM \quad (11)$$

$$K_E = K_T - K_Z \quad (12)$$

where  $A$  stands for APE and  $K$  stands for KE. The suffixes  $T$ ,  $Z$  and  $E$  refer to the total, zonal and eddy forms respectively. The symbols  $[ ]$ ,  $(\bar{\quad})$ ,  $(\overline{\quad})$  denote the areal mean, departure from the areal mean and zonal mean on an isobaric surface.  $\gamma$  is defined as the stability factor by Holopainen (1970) and is a measure of the eddy activity in the atmosphere.  $T$  is temperature,  $u$  and  $v$  are the zonal and meridional components of the wind respectively,  $dM$  is the mass per unit area ( $dM = \rho dz$ ).

## 2.3. Advection of energy

As we are considering only a limited region, it is necessary, as pointed by Smith (1969), to compute the advection of the energy terms. If  $A$  is a scalar parameter whose advection is to be computed, its advection is given by:

$$\int_S \mathbf{V} \cdot \nabla A ds \quad (13)$$

\*Indian Daily Weather Report (1978-79) published by the India Meteorological Department, New Delhi

$$\text{Now, } \int_S \nabla \cdot (\mathbf{V} A) ds = \int_S A \nabla \cdot \mathbf{V} ds + \int_S \mathbf{V} \cdot \nabla A ds$$

$$\text{or, } \int_S \mathbf{V} \cdot \nabla A ds = \int_S \nabla \cdot (\mathbf{V} A) ds - \int_S A \nabla \cdot \mathbf{V} ds \quad (14)$$

where  $\mathbf{V}$  is a vector: wind and  $\nabla$  is the del operator and  $ds = dx dy$ . As the divergence of the geostrophic wind is negligibly small in comparison to the advection term, Eqn. (14) can be written as :

$$\int_S \mathbf{V} \cdot \nabla A ds = \int_S \nabla \cdot (\mathbf{V} A) ds \quad (15)$$

Eqn. (15) shows that the advection of  $A$  is given by the flux term. Using Gauss's divergence theorem one can express this by :

$$\int_S \nabla \cdot (\mathbf{V} A) ds = \oint_L V_n A dL \quad (16)$$

which states that the horizontal flux across the boundary is given by the closed line integral taken around a given curve. Here  $V_n$  is the velocity along the outward directed normal. In this study, the advection of all energy components namely,  $A_Z$ ,  $A_E$ ,  $K_Z$ ,  $K_E$  were computed in this way.

### 3. Discussion of results

#### 3.1. Stability factor

The magnitude of  $\gamma$  is a measure of eddy activity. Fig. 2 represents the mean vertical distribution of  $\gamma$  for case I as well as for case II. From this figure, it is clear that the maximum value of  $\gamma$  lies at about 300 mb in both cases. Smagorinsky (1963) have computed  $\gamma$  for the entire northern hemisphere and their results show that it reaches a maximum around 400 mb. Baker *et al.* (1977) have calculated the values of  $\gamma$  using the data obtained from the NCAR General Circulation Model. Their result shows that the maximum value of  $\gamma$  lies at about 300 mb. Our results are comparable.

#### 3.2. Daily variations of energy

Fig. 3(a) shows vertically integrated daily variation of  $A_Z$ ,  $A_E$ ,  $K_Z$ ,  $K_E$  for 11 to 18 Aug 1978 at 00 GMT. This is case I. The zonal forms of energy ( $A_Z$  and  $K_Z$ ) reach the maximum value on 14 Aug and then start decreasing up to 17 Aug. However, the eddy forms of energy ( $A_E$  and  $K_E$ ) reached a maximum on 15 Aug. There was a low over the head Bay of Bengal on 12 Aug. This intensified into a depression on 13 Aug and was a deep depression by 14/15 Aug. Later, it moved over the adjoining land on 16 Aug and started dissipating subsequently. It merged with the seasonal trough on 18th. The maximum intensity of the depression was on 15 Aug. The eddy form of energy showed a variation similar to the variation in the intensity of the depression. The zonal form also behaved in a similar way, but its maximum was on 14 Aug rather than 15 Aug, although the total potential energy ( $A_Z + A_E$ ) was at a maximum on 15 Aug. The intensity of the depression was so

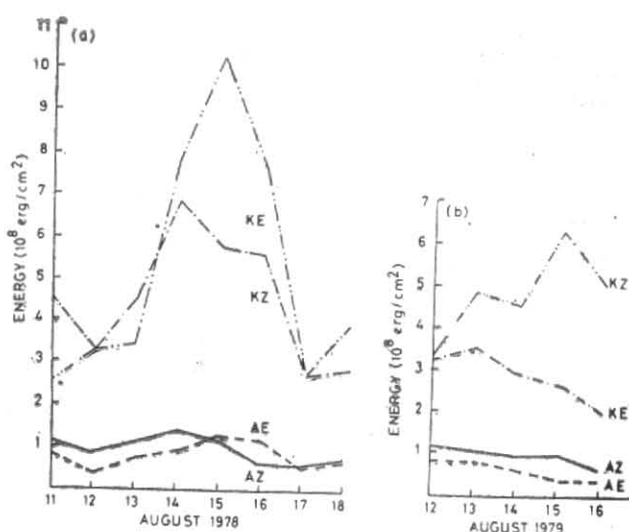


Fig. 3. Day to day variation of the various energy forms for cases I and II

strong that the magnitude of  $A_E$  on 15 Aug exceeded that of  $A_Z$ .

Fig. 3(b) shows the vertically integrated daily variation of energy for case II. This was a weak monsoon situation over the Indian subcontinent. We found that the zonal form of the kinetic energy had an increasing tendency from initial stage. It reached its maximum on 15 Aug. It decreased when the depression merged with the seasonal trough.

The zonal form of the APE does not show any great change from 12 to 15 Aug 1979. Thereafter, it gradually decreased with the dissipation of the depression. The curve of  $A_E$  and  $K_E$  indicated that both lost their energy to the zonal form.

Comparing the results of case I with that for case II we noted that during the mature stage of the depression, both the zonal and eddy forms of the kinetic energy had a similar tendency for case I. But, in case II the zonal and eddy forms of kinetic energy were in opposite phase.

#### 3.3. Advection of energy terms

The advection of energy is shown in Table 1 (a & b). During the strong monsoon epoch, the zonal flux of both  $A_Z$  and  $K_Z$  was directed inward during maturity, otherwise, it showed an outgoing flux during the initial and decaying stages of the depression. The eddy flux of APE was inward throughout the life cycle of the depression, but for the kinetic energy it was directed inward only during the decaying stage.

For a weak monsoon situation, both  $A_Z$  and  $K_Z$  was directed inward throughout the life cycle of the depression. An outgoing flux of eddy available potential energy was observed during the decaying stage, and for kinetic energy it was during the mature stage of the depression.

TABLE 1

Dep. stages	$FAZ$	$FAE$	$FKZ$	$FK_E$
(a) Advection of the energy ( $\text{erg cm}^{-2} \text{ sec}^{-1}$ ) for case I (Aug 1978)				
Initial	$0.23 \times 10^3$	$-0.17 \times 10^3$	$0.54 \times 10^3$	$0.82 \times 10^2$
Mature	$-0.56 \times 10^3$	$-0.56 \times 10^3$	$-0.48 \times 10^3$	$0.57 \times 10^4$
Decay	$0.97 \times 10^2$	$-0.84 \times 10^2$	$0.14 \times 10^4$	$-0.29 \times 10^4$
(b) Advection of the energy ( $\text{erg cm}^{-2} \text{ sec}^{-1}$ ) for case II (Aug 1979)				
Initial	$-0.13 \times 10^3$	$-0.57 \times 10^3$	$-0.33 \times 10^3$	$-0.12 \times 10^4$
Mature	$-0.16 \times 10^3$	$-0.59 \times 10^3$	$-0.22 \times 10^4$	$0.25 \times 10^4$
Decay	$-0.96 \times 10^2$	$0.21 \times 10^2$	$-0.29 \times 10^3$	$-0.13 \times 10^4$

#### 4. Conclusion

From the above discussion we find that for a strong monsoon situation the magnitude of zonal APE was greater than eddy APE during initial and decaying stages. However, during the mature stage, reverse is the case. The magnitude of  $A_E$  exceeded  $A_Z$ . For a weak monsoon case, the zonal APE was always greater than eddy APE throughout the life cycle of the depression. During the mature stage of the depression, zonal and eddy forms of the kinetic energy have a similar tendency for a strong monsoon, but they show an opposite tendency for a weak monsoon.

The magnitude of  $K_Z$  was the same for both the cases. But, the magnitude of  $K_E$  was nearly double for a strong monsoon case, and it was about half that of  $K_Z$  for the weak monsoon situation.

We conclude that the intensity of the monsoon during a depression was associated more with the eddy form of both available and kinetic energy.

#### Acknowledgements

The authors wish to express their sincere thanks to the Director General of Meteorology, India Meteorological Department, New Delhi for providing the necessary data required for the present study. Their grateful thanks are due to the referee whose careful review led to considerable improvement in its presentation.

#### References

- Baker, E.W., Kung, E.C. and Sommerville, C. J., 1977, *Mon. Weath. Rev.*, **105** (11), pp. 1384-1401.
- Holopainen, E.O., 1970, *Quart. J. R. met. Soc.*, **96**, pp. 626-644.
- Kida, H., 1977, *J. met. Soc. Japan*, **55** (1), pp. 52-70.
- Lorenz, E.N., 1955, *Tellus*, **7**, pp. 157-167.
- Shuman, F.G., 1957, *Mon. Weath. Rev.*, **85**, pp. 357-361.
- Smagorinsky, J., 1963, *Mon. Weath. Rev.*, **91**, pp. 99-164.
- Smith, P. J., 1969, *Tellus*, **21**, pp. 202-207.